Am. J. Trop. Med. Hyg., 99(2), 2018, pp. 380–387
doi:10.4269/ajtmh.17-0912
Copyright © 2018 by The American Society of Tropical Medicine and Hygiene

Carotid *Taenia solium* Oncosphere Infection: A Novel Porcine Neurocysticercosis Model

Karen A. Alroy,[1]† Gianfranco Arroyo,[2]† Robert H. Gilman,[1] Eloy Gonzales-Gustavson,[3] Linda Gallegos,[3] Cesar M. Gavidia,[3] Manuela Verastegui,[4] Silvia Rodriguez,[5]‡ Teresa Lopez,[3] Luis A. Gomez-Puerta,[3] Joseph Alroy,[6] Hector H. Garcia,[5]* and Armando E. Gonzalez[5] for the Cysticercosis Working Group in Peru

[1]*Department of International Health, Bloomberg School of Public Health, Johns Hopkins University, Baltimore, Maryland;* [2]*School of Public Health and Management, Universidad Peruana Cayetano Heredia, Lima, Peru;* [3]*School of Veterinary Medicine, Universidad Nacional Mayor de San Marcos, Lima, Peru;* [4]*Departments of Pathology, Universidad Peruana Cayetano Heredia, Lima, Peru;* [5]*Microbiology of the School of Science, Universidad Peruana Cayetano Heredia, Lima, Peru;* [6]*School of Medicine, Tufts University, Boston, Massachusetts*

Abstract. Neurocysticercosis (NCC), the infection of the human central nervous system (CNS) with larval cysts of *Taenia solium* causes widespread neurological morbidity. Animal models are crucial for studying the pathophysiology and treatment of NCC. Some drawbacks of current NCC models include differences in the pathogenesis of the model and wild-type parasite, low rates of infection efficiency and lack of reproducibility. We describe a novel porcine model that recreates infection in the CNS with high efficiency. Activated oncospheres, either in a high (45,000–50,000) or low (10,000) dose were inoculated in the common carotid artery of 12 pigs by ultrasound-guided catheterization. Following oncosphere injection, either a high (30 mL) or low (1–3 mL) volume of saline flush was also administered. Cyst burden in the CNS was evaluated independently according to oncosphere dose and flush volume. Neurocysticercosis was achieved in 8/12 (66.7%) pigs. Cyst burden in the CNS of pigs was higher in the high versus the low oncosphere dose category (median: 4.5; interquartile ranges [IQR]: 1–8 and median: 1; IQR: 0–4, respectively) and in the high versus the low flush volume category (median 5.5; IQR: 1–8 and median: 1; IQR: 0–2, respectively), although not statistically different. All cysts in the CNS were viable, whereas both viable and degenerated cysts were found in the musculature. Carotid injection of activated oncospheres in pigs is effective in reproducing NCC. Oncosphere entry into the CNS by way of vasculature mimics wild-type infection, and provides a useful alternative for future investigations on the pathogenesis and antiparasitic treatment of NCC.

INTRODUCTION

Taenia solium, also referred as the "pork tapeworm," causes taeniasis and cysticercosis, which is considered a neglected zoonotic disease. It is common in many rural areas of developing countries where the lack of sanitation and hygiene conditions, human open-air defecation, and the presence of free-roaming pigs is common.[1,2] The parasite has a two-stage lifecycle, including humans as the definitive host of the intestinal adult tapeworm and pigs as the natural intermediate host of the larval form or cysticercus.[2] Humans develop taeniasis by eating infected pork containing larval cysts, whereas pigs develop cysticercosis in their tissue by ingestion of infective eggs released in the feces of a human tapeworm carrier.[2,3] Humans can also develop cysticercosis when they accidentally ingest eggs by fecal–oral route from a close contact with a tapeworm carrier.[4] Cyst establishment in the central nervous system (CNS) leads to the development of neurocysticercosis (NCC), a debilitating neurological condition considered as the leading cause of late-onset epilepsy in low-income countries.[5,6] This disease has also become an increasing public health concern in industrialized countries, with more than 18,000 cases in the United States, resulting in a negative economic impact due to hospitalization costs.[7]

Clinical manifestations in human NCC can vary from asymptomatic cases to severe illness, and even death.[8] The variety of signs observed reflects the characteristics of the infection in the CNS (stage, number, and location of cysts as well as the host's immune response toward larval cysts).[4] Neurological symptoms include persistent headache, memory loss, hydrocephalus, increased intracranial pressure, and most commonly, the development of seizures and epilepsy.[4,9,10] Antiparasitic therapy can also exacerbate clinical manifestations in NCC, probably as a result of the inflammatory response to antigens released by dying cysts immediately after treatment. Typically, steroids are co-administered with antiparasitic drugs to control the inflammatory response secondary to cyst damage by the immune response, and to reduce the risk of seizures.[11] Further studies are necessary for a better understanding of the pathophysiological processes in NCC, host–parasite interactions, and for improving current therapeutic regimens. In this context, the development of an accurate animal model may be valuable for the study of NCC.

Animal models are critical for studying the processes that occur during the infection course in NCC. An ideal animal model that closely resembles the parasite lifecycle is useful to study the pathophysiological processes that occur during cyst implantation into the CNS, the development of the immune response, and the identification of specific biomarkers for early stages of development.[12] In addition, an animal model with high rates of viable cyst infections in the CNS may allow the control of variables such as infection dose and cyst longevity, especially important in controlled studies for treatment regimens.[13–15] A variety of studies have been performed using pigs[16–20] and rodents[21–24] as NCC animal models, each with their own advantages and disadvantages. We describe a novel experimental porcine NCC model, using ultrasound-guided carotid artery catheterization. By inoculating oncospheres into the carotid artery, the model aims to accurately recreate oncosphere entry into the CNS through the blood–brain barrier. This method would not generate any artifact to brain tissue or meninges due to direct injection of parasites

* Address correspondence to Hector H. Garcia, Department of Microbiology, School of Sciences, Universidad Peruana Cayetano Heredia, Avenida Honorio Delgado 430, SMP, Lima, Peru. E-mail: hgarcia1@jhu.edu
† These authors contributed equally to this work.
‡ Deceased.

into the brain and could potentially reveal important information about early CNS infection, especially how oncospheres gain access into the brain. Our model produces high rates of infection efficiency into the CNS and provides an alternative for further experimental studies.

MATERIALS AND METHODS

Study animals. Twelve mixed-breed pigs 8–11 weeks old, negative to *T. solium* antibodies determined by lentil lectin–bound glycoprotein enzyme-linked immunotransfer blot (LLGP-EITB)[25,26] were purchased from a cysticercosis-free farm in Lima, Peru. Pigs were housed in the veterinary facilities at San Marcos University (FMV-UNMSM), in Lima, Peru, where they were allowed 2 weeks of acclimatization in their new environment. All study procedures were reviewed and approved by the Animal Use and Care Committee of the FMV-UNMSM (Ethics Authorization Number 007), which adheres with the guidelines of the Office of Laboratory Animal Welfare of the National Institutes of Health.

Parasite, oncosphere collection, and inoculum preparation. A total of six adult tapeworm specimens were collected from patients treated with a single oral dose (2 g) of niclosamide.[27] Taenias were collected and stored in Falcon 15-mL tubes containing saline solution with antibiotics (10 U/mL penicillin, 100 µg/mL streptomycin, and 0.25 µg/mL amphotericin B) at 4°C until used (within a 4-week period of collection). Species differentiation (*T. solium* and *Taenia saginata*) was performed by microscopy for morphological characteristics of gravid proglottids (numbers of uterine branches) and scolex (rostellum with hooks in *T. solium*), and confirmed by polymerase chain reaction as previously described.[28]

Eggs were obtained from gravid proglottids by gentle homogenization, washed three times in distilled water (with centrifugation steps between washes of 2,500 × *g* per 5 minutes each), collected, and subsequently exposed for 10 minutes to 0.75% sodium hypochlorite at 4°C for oncosphere hatching as previously described.[29] The supernatant containing oncospheres was centrifuged in RPMI 1640 medium (Sigma Chemical Co., St. Louis, MO), resuspended in the same media, and a sample containing approximately 100 oncospheres was placed in a Neubauer chamber and tested for viability by microscopy using Trypan Blue at 0.4%. Oncospheres were then activated using artificial intestinal fluid (1 g pancreatin [Sigma Chemical Co.], 1 mL pig bile, and 200 mg Na_2CO_3, adjusted to a volume of 100 mL with RPMI medium) by incubation at 37°C for 1 hour as previously described.[29,30] Activated oncospheres were rinsed, resuspended in RPMI medium, counted, and separated in individual inoculums of 1 mL for immediate use within 2 hours.

Infection procedure. Activated oncospheres were inoculated in pigs via catheterization of the common carotid artery as this vessel supplies the cerebral anterior vasculature (see Figure 1). Pigs were anesthetized using a combined intramuscular dose of ketamine (20 mg/kg) plus xylazine (2 mg/kg) for induction and intravenous doses of ketamine (5 mg/kg) every 20 minutes for maintenance. Animals were placed in dorsal recumbency and monitored for anesthetic depth and cardiovascular stability. The ventral section of the neck was sterilized with povidone-iodine at 10% for catheterization. A portable ultrasound device (Micromaxx; Sonosite, Bothell, WA) with a vascular probe was used to visualize the carotid artery on the right side of the neck, and the Seldinger technique[31] was performed for percutaneous catheterization of the artery, using a 22-ga, 10-cm sterile central line venous catheter (Arrow International, Teleflex Int, Reading, PA).

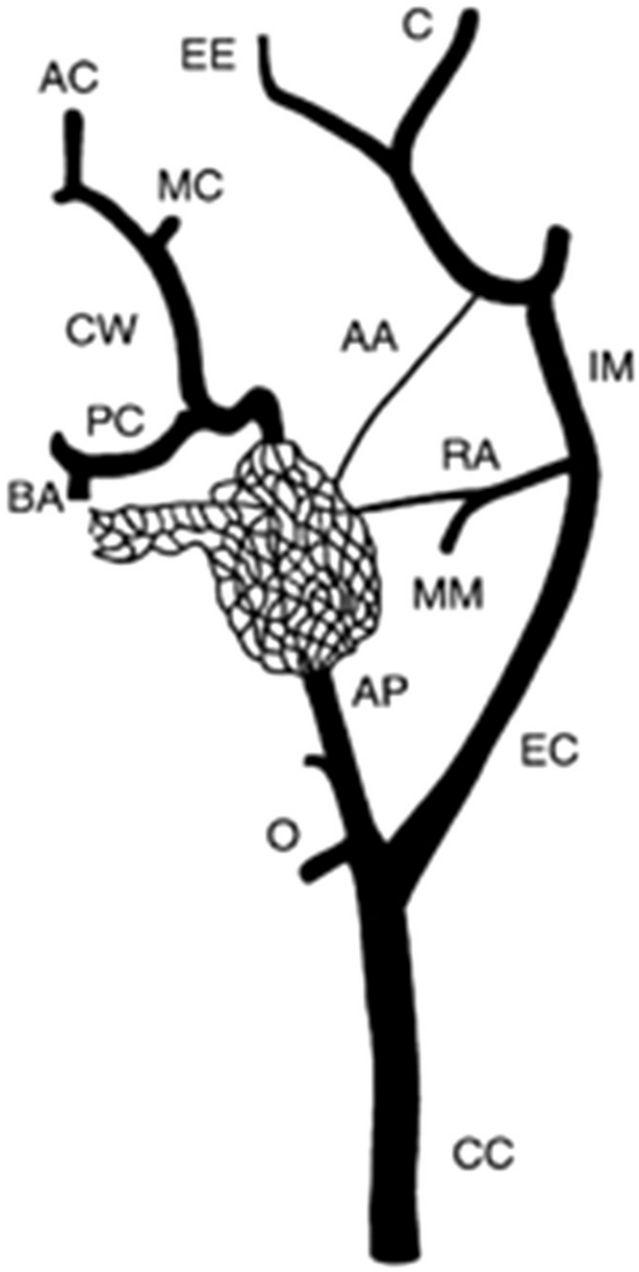

FIGURE 1. Schematic representation of the common carotid artery anatomy of the swine head and neck. The carotid rete mirabile is situated at the termination of the ascending pharyngeal artery. In the swine, the internal carotid artery is very short and joins the rete to the circle of Willis. AA = arteria anastomotica; AC = anterior cerebral artery; AP = ascending pharyngeal artery; BA = basilar artery; C = ciliary artery; CC = common carotid artery; EC = external carotid artery; EE = external ethmoidal artery; IM = internal maxillary artery; MM = middle meningeal artery supplying the ramus anastomoticus; O = occipital artery. Reproduced with permission from the *American Society of Neuroradiology*.[33]

Two variables for oncosphere administration were considered: 1) parasite dosage (number of activated oncospheres administered) and 2) volume of sterile saline flush

post-oncosphere administration. For this, an equal number of pigs were distributed to receive either a high (45,000–50,000) or a low (10,000) oncosphere dose, and in each dose group, an equal number of pigs were also distributed to receive a high (30 mL) or low (1–3 mL) volume of saline flush. Following the administration of the saline flush (either in high or low volume), pigs received a second flush of 5 mL of saline to ensure oncosphere clearance from the catheter.

Clinical and serological monitoring. Pigs were kept in the experimental facilities at FMV-UNMSM for 12 weeks. Clinical status of pigs was checked every day by the veterinary staff. Blood samples were also obtained from the anterior vena cava of pigs on a weekly basis during the study period. Sera aliquots were evaluated for the presence of antibodies by LLGP-EITB,[25,26] and circulating parasite antigens by the B158/B160 monoclonal antibody-based enzyme-linked immunosorbent assay.[32] Antibody levels were expressed as the number of LLGP-EITB bands visualized, with the presence of one or more bands considered as positive. Antigen levels were expressed as the ratio of the optical density of the sample to a cutoff defined by negative control sera; antigen ratios > 1 were considered positive for the presence of circulating antigen.

Necropsy, cyst evaluation, and histopathology. After a period of 12 weeks postinfection (PI), all pigs were euthanized for the assessment of cysts. Pigs were induced to anesthesia with an intramuscular dose of ketamine (20 mg/kg) and xylazine (2 mg/kg), and received an intravenous overdose of sodium pentobarbital (80 mg/kg) for euthanasia. A thorough-gross necropsy was conducted in each carcass, including a complete count of all cysts in brain and muscles. Cysts were classified based on their macroscopic appearance as vesicular (apparently viable cysts with a thin-walled bladder filled with clear fluid and a visible scolex in its interior) and degenerated (soft caseous cysts without clear fluid or visible scolex). All cysts in the brain and brain stem were recorded as a proxy for the CNS; the spinal cord was not evaluated on necropsy. All cysts in the musculature were also recorded. A portion of vesicular cysts in musculature were evaluated for viability by a cyst evagination test as previously described.[17] Cysts within the CNS were additionally evaluated by histopathology to describe inflammatory responses due to cyst establishment. Multiple samples of formalin-fixed tissue containing cysts were embedded in paraffin, and 5-μm sections were stained with hematoxylin and eosin and evaluated by a board-certified veterinary pathologist (J.A.).

Statistical analysis. Viable and degenerated cysts in brain and musculature of pigs were expressed as medians and interquartile ranges (IQRs), according to oncosphere dose and volume of saline flush, evaluated separately, and compared using the Mann–Whitney *U* test. The overall correlation between muscle and brain cysts of pigs was calculated using the Spearman test, and the proportion of viable cysts in the CNS according to oncosphere dose, and volume of saline flush was compared using Fisher's exact test. Antibody and antigen levels were measured at days 0, 45, and 90 PI, expressed as medians and IQRs, and overall correlations between antibody and antigen levels with cyst burden in the CNS and musculature of pigs were also analyzed using the Spearman test. Statistical analyses were performed in R version 3.3.1. *P* values < 0.05 were statistically significant.

RESULTS

A total of six *T. solium* tapeworm specimens, confirmed by microscopy and PCR, were evaluated for oncosphere viability test (see Table 1). Specimens were collected of patients from Lima (*N* = 3), Tumbes (*N* = 1), and Puno (*N* = 2). Oncospheres from all specimens showed percentages of oncosphere viability > 70%, except in one specimen collected from a patient from Puno, with a percentage of oncosphere viability of 55%. The average percentage of oncosphere viability was 73%.

None of the pigs showed neurological signs associated with parasite infection in the CNS during the whole study period. Of the 12 challenged pigs, 10 (83.3%) developed cysts in the musculature, and of these, 8 (66.7%) also developed cysts in the CNS (see Table 2). Two pigs (inoculated with a low oncosphere dose and each receiving a high and a low volume of saline flush) did not develop cyst infection in any organ; these animals were the youngest (8 weeks old during the infection procedure). In the animals with NCC, all CNS cysts were viable, with an overall median number of 5.5 cysts (IQR: 2–7.5 cysts). Cysts were distributed in the brain parenchyma, midbrain, brainstem, or in the subarachnoid spaces (Figure 2A) and no cysts were found in the cerebellum. In the animals with cysticercosis, cysts found in the musculature were both viable and degenerated (Figure 2B), with a median number of 177.5 viable cysts (IQR: 12–942 cysts) and a median of 2.5 degenerated cysts (IQR: 0–28.5 cysts). These cysts were predominantly found in skeletal muscles of the limbs, neck, thorax, and back, as well as in the tongue and heart. Pigs with extra-CNS cysticercosis had no cysts in the tongue; one of these pigs had all its cysts in the muscles of the neck, the majority on the right side. The overall correlation between brain cysts and muscle cysts was 0.78 (*P* value = 0.0026).

A trend toward high cyst burden in the CNS of pigs was observed when comparing a high versus a low oncosphere dose (median: 4.5 cysts; IQR: 1–8 cysts and median: 1 cysts; IQR: 0–4 cysts, respectively; *P* value = 0.2198) and when comparing a high versus low flush volume post-oncosphere inoculation (median: 5.5 cysts; IQR: 1–8 cysts and median: 1 cyst; IQR: 0–2 cysts, respectively; *P* value = 0.1409). Viable cyst burden in the musculature was also higher (but not statistically different) in pigs that received a high oncosphere dose compared with those that received a low oncosphere dose (median: 879.5 cysts; IQR: 127–1,822 cysts and median: 40 cysts; IQR: 0–228 cysts, respectively; *P* value = 0.0542) and in pigs that received a high flush volume versus pigs that received a low flush volume (median: 412 cysts; IQR: 5–822 cysts and median: 151 cysts; IQR: 19–1,062 cysts, respectively; *P* value = 0.9361). Degenerated muscle cyst burden was higher (but not statistically different) in pigs in the low

TABLE 1

Procedure and numbers of *Taenia solium* gravid proglottids collected from tapeworm carriers and percentages of oncosphere activation

Tapeworm number	Patient's location	Numbers of gravid proglottids	Numbers of eggs evaluated	Percentage of oncosphere activation
1	Lima	30	985,000	70
2	Tumbes	13	275,000	70
3	Lima	37	355,000	90
4	Lima	56	745,000	75
5	Puno	16	40,000	55
6	Puno	20	700,000	78

TABLE 2
Detailed cyst burden according to sample tissue and percentage of cyst viability in experimentally infected pigs

Pig ID	Age at infection (weeks)	Oncosphere dose*	Volume of saline flush†	Cysts in the musculature		Cysts in the CNS	Cyst viability (%) evaluated in muscle cysts
				Vesicular	Degenerated	Vesicular	
105	11	High	High	697	0	8	67% (22/33)
101	9	High	High	2,056	4	19	70% (21/30)
6	9	High	High	127	0	1	100% (37/37)
107	11	High	Low	1,062	1	2	78% (31/40)
103	9	High	Low	1,822	41	7	70% (35/50)
9	10	High	Low	19	5	0	100% (17/17)
102	10	Low	High	822	117	7	70.2% (40/57)
106	8	Low	High	0	0	0	–
19	9	Low	High	5	43	4	0% (0/5)
108	9	Low	Low	75	1	0	60% (18/30)
104	8	Low	Low	0	0	0	–
22	9	Low	Low	228	16	2	90.2% (83/92)

CNS = central nervous system.
* High (45,000–50,000 oncospheres) and low (10,000 oncospheres).
† High (30 mL) and low (1–3 mL).

versus the high oncosphere dose category (median: 8.5 cysts; IQR: 0–43 cysts and median: 2.5 cysts; IQR: 0–5 cysts, respectively; *P* value = 0.5676) and similar in the high versus the low flush volume category (median: 2 cysts; IQR: 0–43 cysts and median: 3 cysts; IQR: 1–16 cysts, respectively; *P* value = 0.8065). According to oncosphere dosage, the proportion of viable cysts in the CNS was 0.64% (37/5,820 cysts) in the high dose category and 1.14% (13/1,130 cysts) in the low dose category, and not statistically different (*P* value = 0.082); according to volume of saline flush, the proportion of viable cysts lodged in the CNS was 1.04% (39/3,476 cysts) in the high volume category and 0.34% (11/3,217 cysts) in the low volume category, and statistically different (*P* value = 0.001).

Viable cysts evaluated from muscles showed a 70% mean viability (see Table 2, and Figure 2C). A total of 36 cysts with adjacent tissue were recovered from the brain of the eight NCC pigs and evaluated for histopathology. Histopathological examinations revealed the presence of a cyst, occasionally with cysticercus larvae within it, surrounded by a mixed population of inflammatory cells at the peripheral tissue (Figure 3A). The inflammatory cells included predominantly populations of lymphocytes, plasmatic cells, macrophages, and also eosinophils and neutrophils (Figure 3B). Some macrophages were also arranged in a palisading architecture.

Serological responses in pigs were evaluated at days 0, 45, and 90 PI. All pigs (except those with zero cysts at necropsy) were strongly positive for circulating antigens (antigen ratios > 20) at days 45 and 90 PI (median: 68.8; IQR: 35–73.8 at day 45 PI and median: 73.5; IQR: 36.7–75.2 at day 90 PI) and not statistically different (*P* value = 0.2853). Antibody bands appeared between days 0 and 45 PI, with medians of three bands (IQR: 1–3) and four bands (IQR: 2.5–5) at days 45 and 90 PI (*P* value = 0.1097). The two pigs with zero cysts at necropsy remained negative for antibody and antigen levels for the duration of the study period. Antigen levels strongly correlated with cyst burden in the musculature (R_s: 0.93, *P* value < 0.001) but not with cyst burden in the CNS (R_s: 0.57, *P* value = 0.0535). Conversely, antibody bands significantly correlated with cyst burden in the CNS (R_s: 0.60, *P* value = 0.032) but not with cyst burden in the musculature (R_s: 0.51, *P* value = 0.0922).

DISCUSSION

The development of an animal model is crucial for the study of NCC because it provides valuable tools for a better understanding of the processes that occur during the infection of the human CNS. Our study demonstrated that intracarotid

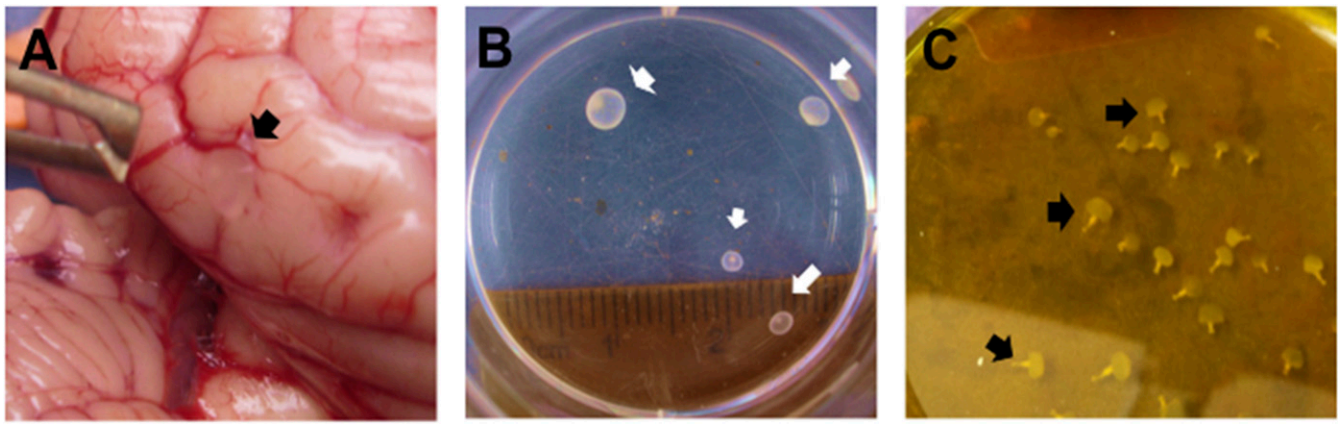

FIGURE 2. Larval cysts recorded in experimentally infected pigs at necropsy. (**A**) Subarachnoid vesicular cyst in situ in the central nervous system of pig with ID 102 (black arrow). (**B**) Vesicular cysts recorded showing a visible scolex in its interior (white arrow). (**C**) Evaginated cysts after incubation with artificial intestinal fluid (black arrows). This figure appears in color at www.ajtmh.org.

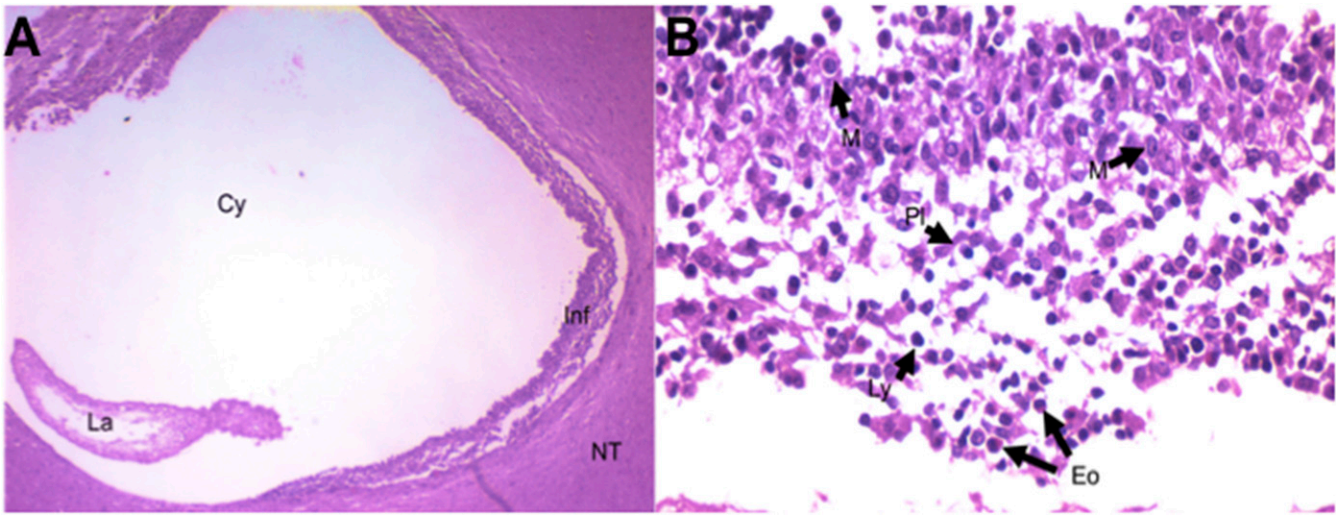

FIGURE 3. Microscopic examination of a *Taenia solium* cyst recovered from the porcine brain. (**A**) Low magnification (×4) of cyst containing a larva (La) inside, with the cerebrum nervous tissue (NT) lined by a mixed inflammatory cell response (Inf). (**B**) Higher magnification (×40) of the inflammatory reaction is oriented with the cyst lumen at the top and the neurologic tissue at the bottom of the histograph. The granuloma is composed of a mixed population of inflammatory cells, including lymphocytes (Ly), plasma cells (Pl), eosinophils (Eo), neutrophils (not illustrated in this section), and macrophages (M). This figure appears in color at www.ajtmh.org.

oncosphere injection in pigs recreates parasite entry into the CNS through the blood–brain barrier and thus provides a reliable method to reproduce NCC.

Experimental oncosphere injection in the vasculature of pigs has been studied previously by Verastegui et al.,[17] showing high rates of cyst infection in the musculature when oncospheres were administered by intravenous route but not cyst infection in the CNS. In our model, we directed the infection toward the CNS by injecting activated oncospheres into the common carotid artery, as this vessel supplies the anterior cerebral vasculature. Unlike humans, before arriving to the circle of Willis, the swine common carotid artery branches into the ascending pharyngeal artery and forms a complex vascular network known as the rete mirabile (Figure 1). Despite the possible barrier effect of the rete mirabile for the oncosphere passage and cyst development in the CNS, we successfully reproduced NCC in 8/12 (66.7%) pigs. Microarteries of the rete mirabile range in the size of 50–250 μm, with an average diameter of 154 μm,[33] thus allowing the passage of oncospheres (typically 30μm in size).[34] Cyst infections were also observed in the musculature of 10/12 (83.3%) pigs. It is likely that a percentage of the inoculum has passed through the external branch of the common carotid artery, and after passing through smaller vessels, the oncospheres established in the musculature and developed into cysts.

All cysts in the CNS of NCC pigs in our model were apparently viable. Similar results have been obtained previously in initial experiments with oral infection with *T. solium* eggs in pigs.[16,18] Oral infection has the advantage of mimicking the wild-type infection route,[12] although to achieve CNS infection with oral infection, a high dose of eggs is necessary (usually 100,000 or more). This implies the need of a large number of *Taenia* specimens, which can be difficult to obtain. Oral infection, although successful to achieve CNS infection, is also limited in its ability to examine the timing and process of oncosphere invasion from the vasculature into the brain. This remains an important gap in knowledge and one that can be studied further with our model. The presence of viable brain cysts in our model also represents an advantage for the study of pathogenesis of inflammatory responses following antiparasitic treatment. In comparison with studies of NCC using naturally infected pigs,[13–15] our model allows to control variables, such as cyst longevity in the CNS, infection dose, and concurrent CNS infections, which may impact the interpretability of different treatment regimens against NCC.

The number of cysts and their distribution in the CNS in our model was quite variable and similar to what is seen in NCC naturally infected pigs, likely reflecting the individual variability of pigs to infection.[35,36] There was also a tendency toward a higher number of cysts in pigs that received a high oncosphere dose or a high volume of saline flush PI. The effect of a higher inoculum on cyst development was similarly observed in previous studies in pigs using oral infection with eggs or intracranial CNS oncosphere injection.[16,18,20] A high flush volume following oncosphere injection in our model may also improve the passage of a greater number of oncospheres through the vasculature toward the CNS. Nonetheless, a lower cyst burden in the CNS, as observed in pigs that received a lower oncosphere dose or lower volume of saline flush, may also be useful to individualize local inflammatory responses in the brain parenchyma. In any case, a high rate of oncosphere viability is necessary to achieve CNS infection, which depends on the protocol of oncosphere activation and the timing between tapeworm collection and oncosphere preparation for use.[17,20,30] The average percentage of viability of the oncospheres used in our model was 73% and correlated with the numbers of cysts observed in muscles and brains of pigs at necropsy. The two animals that did not develop any cysts in their organs were inoculated with the oncospheres collected from the tapeworm from Puno with the lowest percentage of oncosphere viability (55%), which corroborates the importance of oncosphere viability to achieve cyst infection. These pigs were also the youngest (8 weeks at infection), illustrating different results from Deckers et al.[19] who demonstrated that pigs orally infected at a young age (1 month compared with 3 or 5 months) developed a greater number of viable cysts in the musculature.

Both gross and histologic characterization of brains in infected animals were similar to that observed in pigs that naturally acquired NCC[37–40] and included mixed populations of inflammatory cells (lymphocytes, plasma cells, macrophages, and eosinophils) in slice sections of brains. It has been proposed that this proliferation of inflammatory cells from the peripheral circulation is due to an increased permeability of the blood–brain barrier.[41] The inflammatory response seen in the porcine brains is also similar to those observed in human NCC, only differing in a higher number of eosinophils in the pig model. This difference, however, may be influenced by the fact that CNS cyst infection in humans is generally considered more chronic compared with NCC in pigs.[42] Rodents have also been used as animal models to characterize the inflammatory responses in NCC. Cardona et al.[21] reported the development of NCC in the brain of mice after intracranial infection of the cestode *Mesocestoides corti*. *Taenia crassiceps*, another cestode related to *T. solium*, has been used to infect mice intraperitoneally for the study of markers associated with granuloma formation.[22] More recently, Moura et al.[23] developed ventricular NCC in mice by injecting cysticerci of *T. crassiceps* into the CNS of mice. These models are successful in studying the immune response following CNS infection; however, a major drawback of these models is that cyst establishment into the CNS is not part of the wild-type pathology of *M. corti* and *T. crassiceps*. Intracranial injection of activated oncospheres of *T. solium* in rats has been successful in reproducing NCC.[24] Inflammatory responses in the rat brain closely resemble those in human NCC, and rats also develop epilepsy.[24] Intracranial injection, however, does not resemble the parasite's natural infection cycle, and more importantly, a possible mass effect associated with cyst implantation in the small brains of rats can occur. Surgical oncosphere implantation in the brain of pigs has also proven to reproduce CNS infection,[20] although the presence of degenerated cysts in the CNS of this model may indicate an exacerbated inflammatory response associated with surgical implantation of parasites, a disadvantage for this approach.

The overall increase in antigen and antibody levels in sera of pigs following intracarotid oncosphere injection clearly demonstrates the processes of cyst establishment in organ tissues and immune responses toward cysts. Circulating antigen levels in sera mostly correlated with muscle cysts because of a higher cyst burden in the musculature compared with the CNS of infected pigs. Higher numbers of EITB antibody bands have been observed in human NCC,[43,44] similar to the antibody levels in all NCC pigs in our study, although these results may also represent a strong systemic immune response toward muscle cysts.[45] It is likely that antigen levels measured in cerebrospinal fluid (CSF) better correlate with cyst burden in the CNS, as parasite antigens locally produced in the brain tissue are directly released in the CSF. Similarly, antibody levels measured in the CSF may represent their "de novo" synthesis in the CNS or their passive diffusion from the blood system.

Some drawbacks of our study deserve consideration. To achieve cyst infection, we used a high oncosphere dose (as many as 50,000 oncospheres), which can be difficult and inconsistent for many laboratories to obtain. Most studies use 500–1,000 oncospheres via injection in the CNS for infection, so further studies are necessary to optimize the numbers of active oncospheres needed for infection using this technique. Comparisons of cyst burden according to oncosphere dosage and volume of saline flush had limited statistical power, although a trend toward higher cyst burden in the CNS was observed in pigs that received a high oncosphere dose and high volume of saline flush. Comparisons may also be biased as the two pigs without cyst infection in the low oncosphere dose category received the inoculum with the lowest percentage of oncosphere activation (55%), although the analysis excluding these animals showed similar trends between dose categories. There is also a potential technical difficulty during catheter placement and possible extravascular oncosphere inoculation, as observed in one of the pigs that had 100% of the cyst burden implanted in the musculature of the neck. Further experiments are additionally necessary to evaluate model reproducibility and to reduce potential adverse effects of the rete mirabile on CNS infection efficiency. In summary, the experimental porcine NCC model described here efficiently reproduced CNS viable cyst infections and provides a useful alternative for future studies on NCC.

Received November 22, 2017. Accepted for publication March 22, 2018.

Published online June 11, 2018.

Acknowledgments: We thank Erika Perez and Karen Arteaga from the Cysticercosis Unit at the Instituto Nacional de Ciencias Neurologicas (INCN, Lima, Peru) for Western blot processing, Yesenia Castillo from the Department of Microbiology, School of Sciences, Universidad Peruana Cayetano Heredia (UPCH, Lima, Peru) for Ag-ELISA processing, and Elton K. Sanchez from the School of Veterinary, San Marcos University (UNMSM, Lima, Peru) for blood sampling and necropsies. We additionally thank Avi Smith from the School of Medicine, Tufts University (Boston, MA) for his assistance with the histopathology.

Financial support: This study was supported by the Fogarty International Center at the National Institutes of Health (NIH, training grants numbers D43TW008273-05 and D42TW001140) and by Fogarty International Clinical Research Scholars and Fellows Program at Vanderbilt University (grant number R24 TW007988).

Disclaimer: Funders had no role in the study design, experimental phase, analysis, interpretation, in writing the manuscript, or in the decision to submit the manuscript. Contributions to this manuscript by Karen A. Alroy were done in her personal capacity. The information presented does not necessarily reflect the view of the Centers for Disease Control and Prevention, the Department of Health and Human Services, or the United States government.

Authors' addresses: Karen A. Alroy, Centers for Disease Control and Prevention, Atlanta, GA, E-mail: kalroy01@gmail.com. Gianfranco Arroyo, School of Public Health and Management, Universidad Peruana Cayetano Heredia, Lima, Peru, E-mail: arroyogianfranco@gmail.com. Robert H. Gilman, Department of International Health, Bloomberg School of Public Health, Johns Hopkins University, Baltimore, MD, E-mail: gilmanbob@gmail.com. Eloy Gonzales-Gustavson, Linda Gallegos, Cesar M. Gavidia, Teresa Lopez, Luis A. Gomez-Puerta, and Armando E. Gonzalez, School of Veterinary Medicine, Universidad Nacional Mayor de San Marcos, Lima, Peru, E-mails: gonzaleseloy@yahoo.com, linda.gallegoschu@gmail.com, cgavidiac@unmsm.edu.pe, teresalopezup@gmail.com, lucho92@yahoo.com, and agonzalezz@gmail.com. Manuela Verastegui, Department of Pathology, School of Sciences, Universidad Peruana Cayetano Heredia, Lima, Peru, E-mail: manuela.verastegui@upch.pe. Joseph Alroy, School of Medicine, Tufts University, Boston, MA, E-mail: joealroy@gmail.com. Hector H. Garcia, Department of Microbiology, School of Sciences, Universidad Peruana Cayetano Heredia, Lima, Peru, E-mail: hgarcia1@jhu.edu.

REFERENCES

1. Gilman RH, Gonzalez AE, Llanos-Zavalaga F, Tsang VC, Garcia HH; Cysticercosis Working Group in Peru, 2012. Prevention and control of *Taenia solium* taeniasis/cysticercosis in Peru. *Pathog Glob Health 106:* 312–318.

2. Gripper LB, Welburn SC, 2017. Neurocysticercosis infection and disease—a review. *Acta Trop 166:* 218–224.
3. Coral-Almeida M, Gabriel S, Abatih EN, Praet N, Benitez W, Dorny P, 2015. *Taenia solium* human cysticercosis: a systematic review of sero-epidemiological data from endemic zones around the world. *PLoS Negl Trop Dis 9:* e0003919.
4. Garcia HH, Nash TE, Del Brutto OH, 2014. Clinical symptoms, diagnosis, and treatment of neurocysticercosis. *Lancet Neurol 13:* 1202–1215.
5. Nash TE, Garcia HH, 2011. Diagnosis and treatment of neurocysticercosis. *Nat Rev Neurol 7:* 584–594.
6. Coyle CM et al., 2012. Neurocysticercosis: neglected but not forgotten. *PLoS Negl Trop Dis 6:* e1500.
7. O'Neal SE, Flecker RH, 2015. Hospitalization frequency and charges for neurocysticercosis, United States, 2003–2012. *Emerg Infect Dis 21:* 969–976.
8. Carabin H, Ndimubanzi PC, Budke CM, Nguyen H, Qian Y, Cowan LD, Stoner JA, Rainwater E, Dickey M, 2011. Clinical manifestations associated with neurocysticercosis: a systematic review. *PLoS Negl Trop Dis 5:* e1152.
9. Montano SM, Villaran MV, Ylquimiche L, Figueroa JJ, Rodriguez S, Bautista CT, Gonzalez AE, Tsang VC, Gilman RH, Garcia HH; Cysticercosis Working Group in Peru, 2005. Neurocysticercosis: association between seizures, serology, and brain CT in rural Peru. *Neurology 65:* 229–233.
10. Gripper LB, Welburn SC, 2017. The causal relationship between neurocysticercosis infection and the development of epilepsy—a systematic review. *Infect Dis Poverty 6:* 31.
11. Garcia HH, Del Brutto OH; Cysticercosis Working Group in Peru, 2017. Antiparasitic treatment of neurocysticercosis—the effect of cyst destruction in seizure evolution. *Epilepsy Behav 76:* 158–162.
12. Arora N, Tripathi S, Kumar P, Mondal P, Mishra A, Prasad A, 2017. Recent advancements and new perspectives in animal models for neurocysticercosis immunopathogenesis. *Parasite Immunol 39:* e12439.
13. Guerra-Giraldez C et al.; Cysticercosis Working Group in Peru, 2013. Disruption of the blood-brain barrier in pigs naturally infected with *Taenia solium*, untreated and after anthelmintic treatment. *Exp Parasitol 134:* 443–446.
14. Mahanty S et al.; Cysticercosis Working Group in Peru, 2015. Post-treatment vascular leakage and inflammatory responses around brain cysts in porcine neurocysticercosis. *PLoS Negl Trop Dis 9:* e0003577.
15. Mahanty S, Orrego MA, Cangalaya C, Adrianzen MP, Arroyo G, Calcina J, Gonzalez AE, Garcia HH, Guerra-Giraldez C, Nash TE; Cysticercosis Working Group in Peru, 2017. TNF-α blockade suppresses pericystic inflammation following anthelmintic treatment in porcine neurocysticercosis. *PLoS Negl Trop Dis 11:* e0006059.
16. de Aluja AS, Villalobos AN, Plancarte A, Rodarte LF, Hernandez M, Sciutto E, 1996. Experimental *Taenia solium* cysticercosis in pigs: characteristics of the infection and antibody response. *Vet Parasitol 61:* 49–59.
17. Verastegui M, Gonzalez A, Gilman RH, Gavidia C, Falcon N, Bernal T, Garcia HH, 2000. Experimental infection model for *Taenia solium* cysticercosis in swine. Cysticercosis Working Group in Peru. *Vet Parasitol 94:* 33–44.
18. Santamaria E, Plancarte A, de Aluja AS, 2002. The experimental infection of pigs with different numbers of *Taenia solium* eggs: immune response and efficiency of establishment. *J Parasitol 88:* 69–73.
19. Deckers N, Kanobana K, Silva M, Gonzalez AE, Garcia HH, Gilman RH, Dorny P, 2008. Serological responses in porcine cysticercosis: a link with the parasitological outcome of infection. *Int J Parasitol 38:* 1191–1198.
20. Fleury A et al., 2015. *Taenia solium*: development of an experimental model of porcine neurocysticercosis. *PLoS Negl Trop Dis 9:* e0003980.
21. Cardona AE, Restrepo BI, Jaramillo JM, Teale JM, 1999. Development of an animal model for neurocysticercosis: immune response in the central nervous system is characterized by a predominance of gamma delta T cells. *J Immunol 162:* 995–1002.
22. Patil S, Robinson P, Actor JK, Baig S, White AC Jr., 2006. Proinflammatory cytokines in granulomas associated with murine cysticercosis are not the cause of seizures. *J Parasitol 92:* 738–741.
23. Moura VB, Lima SB, Matos-Silva H, Vinaud MC, Loyola PR, Lino RS, 2016. Cellular immune response in intraventricular experimental neurocysticercosis. *Parasitology 143:* 334–342.
24. Verastegui MR et al., 2015. Novel rat model for neurocysticercosis using *Taenia solium*. *Am J Pathol 185:* 2259–2268.
25. Gonzalez AE et al., 1990. Prevalence and comparison of serologic assays, necropsy, and tongue examination for the diagnosis of porcine cysticercosis in Peru. *Am J Trop Med Hyg 43:* 194–199.
26. Tsang VC, Pilcher JA, Zhou W, Boyer AE, Kamango-Sollo EI, Rhoads ML, Murrell KD, Schantz PM, Gilman RH, 1991. Efficacy of the immunoblot assay for cysticercosis in pigs and modulated expression of distinct IgM/IgG activities to *Taenia solium* antigens in experimental infections. *Vet Immunol Immunopathol 29:* 69–78.
27. Jeri C, Gilman RH, Lescano AG, Mayta H, Ramirez ME, Gonzalez AE, Nazerali R, Garcia HH, 2004. Species identification after treatment for human taeniasis. *Lancet 363:* 949–950.
28. Mayta H, Gilman RH, Prendergast E, Castillo JP, Tinoco YO, Garcia HH, Gonzalez AE, Sterling CR; Cysticercosis Working Group in Peru, 2008. Nested PCR for specific diagnosis of *Taenia solium* taeniasis. *J Clin Microbiol 46:* 286–289.
29. Verastegui M et al.; Cysticercosis Working Group in Peru, 2007. *Taenia solium* oncosphere adhesion to intestinal epithelial and Chinese hamster ovary cells in vitro. *Infect Immun 75:* 5158–5166.
30. Chile N et al.; Cysticercosis Working Group in Peru, 2016. In vitro study of *Taenia solium* postoncospheral form. *PLoS Negl Trop Dis 10:* e0004396.
31. Swindle M, 2007. *Swine in the Laboratory: Surgery, Anesthesia, Imaging and Experimental Techniques*, 2nd edition. Boca Raton, FL: CRC Press, 195–295.
32. Chembensofu M et al., 2017. Re-visiting the detection of porcine cysticercosis based on full carcass dissections of naturally *Taenia solium* infected pigs. *Parasit Vectors 10:* 572.
33. Massoud TF, Vinters HV, Chao KH, Vinuela F, Jahan R, 2000. Histopathologic characteristics of a chronic arteriovenous malformation in a swine model: preliminary study. *AJNR Am J Neuroradiol 21:* 1268–1276.
34. Pawlowski Z, 2002. *Taenia solium*: basic biology and transmission. Singh G, Prabhakar S, eds. Taenia solium *Cysticercosis: From Basic to Clinical Science*. Wallingford, United Kingdom: CABI Publishing, 1–13.
35. Prasad KN, Chawla S, Prasad A, Tripathi M, Husain N, Gupta RK, 2006. Clinical signs for identification of neurocysticercosis in swine naturally infected with *Taenia solium*. *Parasitol Int 55:* 151–154.
36. Phiri IK, Dorny P, Gabriel S, Willingham AL 3rd, Sikasunge C, Siziya S, Vercruysse J, 2006. Assessment of routine inspection methods for porcine cysticercosis in Zambian village pigs. *J Helminthol 80:* 69–72.
37. Gonzalez D, Rodriguez-Carbajal J, Aluja A, Flisser A, 1987. Cerebral cysticercosis in pigs studied by computed tomography and necropsy. *Vet Parasitol 26:* 55–69.
38. Flisser A et al., 1990. Praziquantel treatment of porcine brain and muscle *Taenia solium* cysticercosis. 1. Radiological, physiological and histopathological studies. *Parasitol Res 76:* 263–269.
39. Londono DP, Alvarez JI, Trujillo J, Jaramillo MM, Restrepo BI, 2002. The inflammatory cell infiltrates in porcine cysticercosis: immunohistochemical analysis during various stages of infection. *Vet Parasitol 109:* 249–259.
40. Mkupasi EM, Ngowi HA, Sikasunge CS, Leifsson PS, Johansen MV, 2014. Distribution and histopathological changes induced by cysts of *Taenia solium* in the brain of pigs from Tanzania. *J Helminthol 6:* 1–6.
41. Cangalaya C et al.; Cysticercosis Working Group in Peru, 2016. Perilesional inflammation in neurocysticercosis—relationship between contrast-enhanced magnetic resonance imaging, Evans blue staining and histopathology in the pig model. *PLoS Negl Trop Dis 10:* e0004869.
42. Alvarez JI, Londono DP, Alvarez AL, Trujillo J, Jaramillo MM, Restrepo BI, 2002. Granuloma formation and parasite

disintegration in porcine cysticercosis: comparison with human neurocysticercosis. *J Comp Pathol 127:* 186–193.

43. Rodriguez S, Dorny P, Tsang VC, Pretell EJ, Brandt J, Lescano AG, Gonzalez AE, Gilman RH, Garcia HH; Cysticercosis Working Group in Peru, 2009. Detection of *Taenia solium* antigens and anti-*T. solium* antibodies in paired serum and cerebrospinal fluid samples from patients with intraparenchymal or extraparenchymal neurocysticercosis. *J Infect Dis 199:* 1345–1352.
44. Zea-Vera A et al.; Cysticercosis Working Group in Peru, 2013. Parasite antigen in serum predicts the presence of viable brain parasites in patients with apparently calcified cysticercosis only. *Clin Infect Dis 57:* e154–e159.
45. Gavidia CM, Verastegui MR, Garcia HH, Lopez-Urbina T, Tsang VC, Pan W, Gilman RH, Gonzalez AE; Cysticercosis Working Group in Peru, 2013. Relationship between serum antibodies and *Taenia solium* larvae burden in pigs raised in field conditions. *PLoS Negl Trop Dis 7:* e2192.